

Nanostructured gold layers. II. Gold deposition onto polystyrene substrate

I. ZGURA, T. BEICA, S. FRUNZA, O. RASOGA, A. GALCA, L. FRUNZA*,
A. MOLDOVAN^a, M. DINESCU^a, C. ZAHARIA^b

National Institute of Materials Physics

^a*National Institute for Laser, Plasma and Radiation Physics*

^b*Institute of Virology St. S. Nicolau of the Romanian Academy*

In the aim to improve the adherence of the nanostructured gold layers onto glass substrate, gold deposition has been first time performed onto a polystyrene (PS) layer. The PS layer of ca. 50nm was spin-coated onto glass plates from a toluene solution. Gold layers of 10-20nm were vacuum deposited at small incidence angle. We found that at variance from the plates with gold deposited directly on the glass, the plates with an intermediate PS layer do not peel under overnight treatment in ethanol solution. The layers were characterized by several methods. X-ray diffraction (XRD) measurements showed that gold peaks have the position corresponding to the face-centered cubic structure: However, the crystallites on the sample with PS layer seem to be a little bit smaller than those with gold deposited directly onto the glass. XR reflectometry measurements have given the thickness of the gold layer in good agreement with the value estimated from quartz monitor readings and with the ellipsometric data as well. Liquid crystal cells were obtained to observe the molecular alignment imposed by the nanostructured gold layer deposited onto PS film. A rather strong interaction of gold atoms with the substrate molecules can be considered on the basis of the XRD and ellipsometry measurements.

(Received November 4, 2009; accepted February 18, 2010)

Keywords: Nanostructured gold layer, Vacuum deposition, Polystyrene substrate, Alignment of liquid crystals

1. Introduction

Self-assembled monolayers (SAMs) can be formed from alkanethiols on the surface of gold, either as single crystals or films [1-4]; these monolayers can further specifically bind proteins. If these bonds are formed in the presence of aligned liquid crystal (LC) molecules, the alignment is disturbed and thus reports the presence of the proteins [5-8].

In the previous work of the series we have established the experimental conditions for the deposition of gold layers on the glass plate surface by vaporization at small angle (large angle with the normal direction) forming nanostructured columnar semi-transparent layers [9]. Correlations were found among the deposition conditions in the particular installation used in the experiments allowing to obtain two-dimensional diagrams (nomograms) designed to let the approximate graphical computation of such conditions in different applications. The layers were characterized and additionally supported by observing the molecular alignment given in the liquid crystal cells obtained with these gold layers.

However, the nanostructured gold layers obtained directly onto the glass support have a rather short life (up to weeks) when stored under open dry atmosphere and even shorter under humid atmosphere or in watery solutions. Literature gives some keys to improve the gold adherence to the glass among which there is the deposition of certain substrates [10-12]. In spite of this, the new intermediate layer complicates the technology of nanostructured gold

deposition and/or may lead to decreasing the optical transmission in functionalized liquid crystal cells.

To improve the adherence of the nanostructured gold layer on glass and to avoid additional metallic depositions we have used organic films containing benzene rings since they might interact with gold through their π -electrons and the bonds [13] might be energetically favorable to stick the gold clusters. In addition, these organic films have the advantage of less significant optical absorbance in the visible spectrum than the supplementary metallic ones. This work reports the use of polystyrene (PS) layers deposited on the glass plates by spin coating from the polymeric solution a technique already developed in our laboratory [14,15]. The gold nanostructured layers deposited over polystyrene are characterized by several methods including the observation of the molecular alignment given in the liquid crystal cells. A rather strong interaction of gold atoms with the substrate molecules was inferred.

2. Experimental

Vapor deposition at oblique incidence was performed with the Hochvakuum B30.2 equipment (Dresden, Germany) previously described [9] together with the deposition conditions. The deposition thickness of the layer was estimated by using oscillating quartz monitor. The glass plates compatible with the two types of sample supports were of 32x23x3mm size.

Gold deposition has been made at the angles which resulted by analyzed nomograms, either onto glass (G) (the layer succession is further noted Au/G) or onto an intermediate polystyrene (PS) film (the layer succession is noted Au/PS/G). Details (the incidence angle of gold deposition θ and the thickness T of the gold layer) about the deposited plates studied here are given in Table 1. Several (up to 32) samples can be obtained in a batch under the same deposition conditions shown in Table 1. In fact, the deposition parameters can have very small deviations from the intended values due to the deposition geometry as it was previously discussed [9].

Polystyrene layers were deposited onto glass plates [14,15] by spin coating with a solution of atactic polystyrene 1.5wt% in toluene, at 3000rpm. Then the covered plates were slowly dried.

Table 1. Parameters of gold deposition onto different substrates.

Sample batch	Layer succession	θ /degree	T* /nm
P(1)	Au/G	80	12
P(2)	Au/PS/G	80	10
P(3)	Au/PS/G	60	20
P(4)	Au/PS/G	60	10
P(5)	Au/G	60	20
P(7)	Au/PS/G	40	20
P(8)	Au/G	80	12
P(9)	Au/G	60	10
	Au/PS/G		

*estimated from the quartz monitor indications.

To characterize the structure and thickness of the deposited layers, several analysis methods were applied. Atomic force microscopy (AFM) investigations used an equipment XE-100 (Park Systems) in non-contact mode. X-ray diffraction (XRD) measurements were done with an equipment D8 Advance (Bruker-AXS) at a grazing angle incidence of 3° , the measuring domain was $5\text{-}65^\circ$, the collecting step was chosen of 0.02° . X-ray reflectometry measurements were performed as well under the same conditions. The equipment for spectro-ellipsometric investigations was a DUV-VIS-XNIR Variable Angle Spectroscopic Ellipsometer (Woollam); the spectral domain spreads between 193 and 2200nm and three incidence angles (65° , 70° , 75°) were set to measure the ellipsometric angles ψ and Δ , on each sample. A simple slab model was then used to interpret these constants.

Liquid crystals symmetric cells with gold layer similarly deposited on both plates and always toward the cell inside were then obtained from the deposited glass plates in order to follow up the effect of the topography anisotropy on the LC alignment. The two glass plates were arranged so that the evaporation/deposition direction was anti-parallel (see Fig. 1): Main evaporation direction and possible orientational directions of the LC molecules (A, B, H and P) are there shown. A, B and H are in the evaporation plane while P is perpendicular onto this plane.

The cell thickness was $15\mu\text{m}$ (by Mylar spacer). For all samples, the plates were held together at two opposed ends using bulldog clips especially during the handling of the cells. The liquid crystal was 4*n*-pentyl-4'-cyanobiphenyl (5CB) from Merck, having transition temperature 35.4°C . It was introduced into the cell in the isotropic state (at 40°C) by capillary action. The cell was then cooled to room temperature. During the cooling process, 5CB changed from its isotropic state to its nematic state. The optical appearance of the sample was observed in transmission mode by direct visualization under crossed polarizers or by conoscopic method (under crossed polarizers and convergent light) using a polarized light microscope (Leitz Orthoplan) with a digital camera (Panasonic DMC-FZ8). Consistent settings of both the microscope light source (numerical aperture 0.6) and the digital camera allowed for the direct comparison of images taken of different samples.

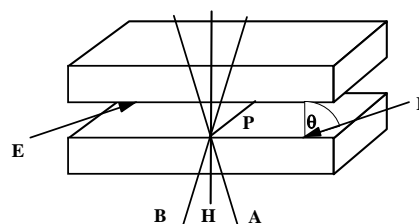


Fig. 1. Two deposited glass plates assembled in a liquid crystal cell. Main evaporation direction E and possible orientational directions of the LC molecules (A , B , H and P) are shown.

3. Results and discussion

3.1 Adherence of gold nanostructured layer to the glass substrate

Gold vapor vacuum deposition directly on the glass plates does not allow obtaining nanostructured layers with good adherence. In Fig. 2, some examples of peeling of the gold nanostructured layer can be observed. After 16 hours of contact with ethanol, both sample types P(8) and P(5) peel off; the samples of P(5) batch with a thicker gold layer peel as compact flakes (downpart of Fig. 2).

At variance from the plates with gold deposited directly on the glass, the plates with an intermediate PS layer do not peel under the above conditions.

3.2 Gold layers onto polystyrene substrate

The thickness of the layers was analyzed by spectroscopic ellipsometry. Polarization direction s is perpendicular on the propagation direction and parallel to the sample surface. Polarization direction p is perpendicular on the propagation direction and is contained in the incidence plane. The representative spectra at one of the used incidence angles of the light are presented in fig. 3 for samples of the batch P(2).

The characteristics of successive layers were obtained by fitting the experimental results. In the case of the samples with PS layer, the best fit included the fit of the optical constants as well, showing that gold interacts rather strongly with the polystyrene substrate. The obtained thickness values are given in Table 2.

Table 2. Thickness (in nm) of the layers from ellipsometry measurements

Layer	Sample batch	
	P(2)	P(4)
Polystyrene	51.2	50.9
Gold	7.3	9.1

One can observe that the PS layer has ca. 50nm while the gold layer has a thickness close to the value estimated from quartz monitor indications.

XRD investigations at small incidence angles have shown the presence of gold (micro)crystallized (see Fig. 4). The broad peak at 24.70° belongs to the amorphous glass. In the case of gold deposited directly onto the glass substrate, there is a good match in the positions and in the intensity ratios with the bulk face-centered cubic gold structure. Thus, the peak at $2\theta=38.23^\circ$, is due to Au(111) and that at $2\theta=44.31^\circ$, to Au(200); the small Au(222) peak is visible toward 65° . However, the diffraction pattern of the gold deposited onto polystyrene has a (111) peak smaller but a little bit broader (see the inset of Fig. 4) than that measured on glass. Besides, the intensity ratio of the Au(111) and Au(200) peaks is lower than in the case of typical face-centered cubic bulk Au, indicating somehow a preferential orientation of gold crystallites onto the sample surface. These results likely reflect the effect of the polystyrene underlayer on the orientation of the gold and indicate that qualitative differences do exist between the crystallographic orientations of the gold layers prepared in different manners.

The significant broadness of the scattering XRD peaks was caused by the very small size of crystallites; the smallest are obtained when deposition took place onto PS layer.

X-ray reflectometry measurements have given the thickness of the gold layer in a rather good agreement with the value estimated from quartz monitor readings.

To characterize the gold films at a resolution of nanometer scale, we applied atomic force microscopy. Figs. 5 give representative AFM images of an obliquely deposited film of gold of the sample batch P(9) either directly onto the glass plate or over an intermediate PS layer. The surface is rough and consisted of easily

visualized grains of gold crystalline with diameters of roughly a few tens of nm. The scale of contrast in the real-space images corresponds to a variation in height (z-axis) of 5nm.

To characterize the roughness quantitatively [16], the contour lengths across a family of directions relative to the direction of gold deposition were measured with different sample lengths. Figs. 6 show examples of the cross-section profile of the roughness scanning across the direction parallel to the direction of gold deposition in the case of the samples mentioned in Fig. 5. Importantly, the contour lengths are longer in the direction parallel to the gold deposition than perpendicular to the gold deposition. The roughness values estimated from AFM measurements are given in Table 3. These results indicate that the topography of surface on an obliquely deposited gold film bears a maximum roughness in the direction parallel to the direction of gold deposition and a minimum roughness in the direction perpendicular to the direction of gold deposition. On the other hand, the different values for the Au/G and Au/PS/G samples in Table 3 correlate with the results of XRD measurements showing that the latter sample type has smaller crystallites asking for smaller roughness.

Table 3. Roughness (in nm) of the gold layers by AFM measurements

Samples P(9)	Direction of evaporation	
	Parallel	Perpendicular
Au/G	3.4	2.7
Au/PS/G	2.7	2.2



Fig. 2. Peeling of the gold layer deposited directly on the glass plates of the same batch after overnight contact with ethanol. Up: samples of the P(8) batch; down: samples of P(5) batch. The black sign on the glass back comes from the initial mark of the plates.

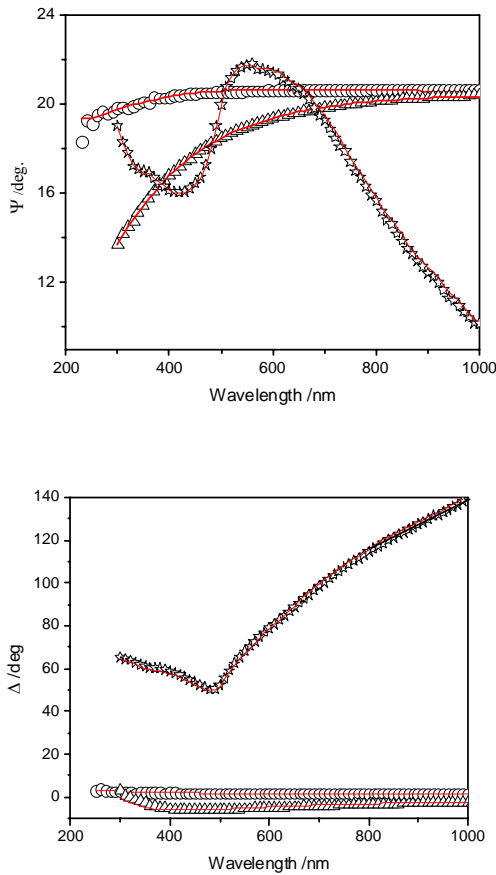


Fig. 3. Ellipsometric constants vs. wavelength for the sample P(2) in different steps of layer deposition as follows: (empty circle) – initial glass, (empty up triangle) – polystyrene layer, (empty star) – Au layer. The solid lines (viewed in red in the online issue) are the model fit. The incidence angle was 70°.

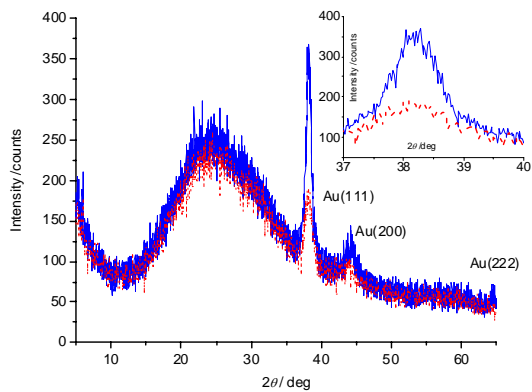


Fig. 4. XRD patterns of the samples type P(5) (solid line) and P(7) (dotted line). In the online issue, the lines are colored. The inset enlarged the region of the Au(111) peak of the two samples.

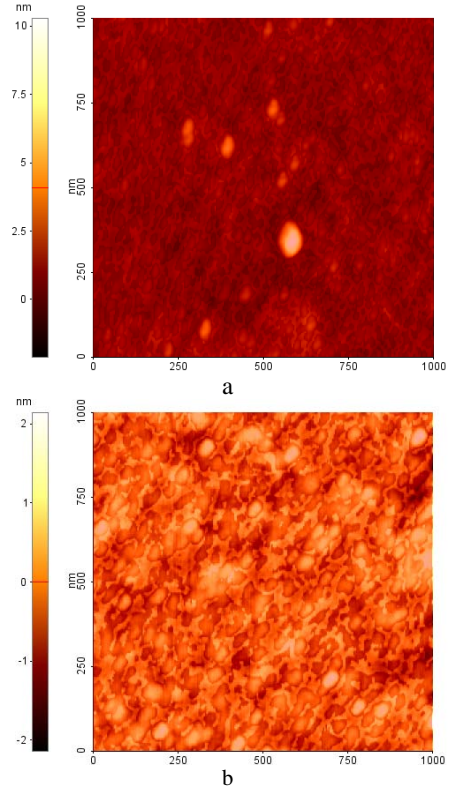


Fig. 5. AFM images of the nanostructured gold layer of the sample batch P(9) deposited onto A) glass; B) a PS layer. The image size is 1 × 1 μm.

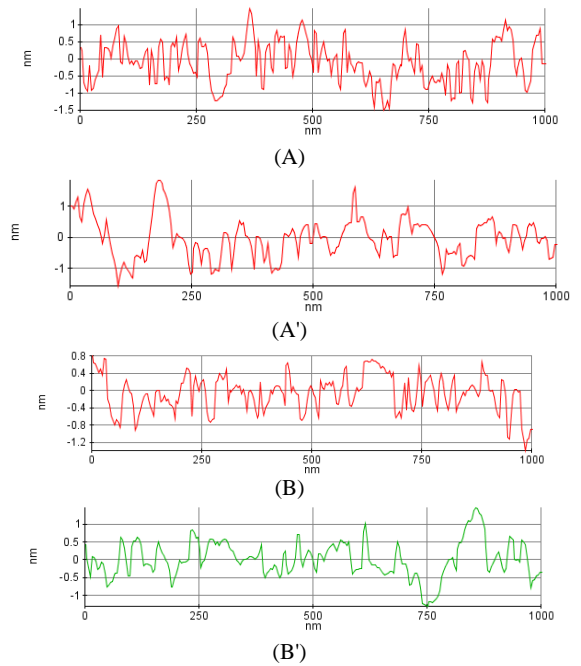


Fig. 6. Line profile of the sample batch P(9) deposited onto A, A') glass; B, B') a PS layer. The profile is scanned across a direction as follows: A, B) parallel to the direction of gold deposition; A', B') perpendicular to the direction of gold deposition.

Gold-polystyrene interaction as demonstrated by our XRD and ellipsometric measurements was expected. As noted in the introduction, benzene rings can interact by their π -electrons with the gold atoms [13]. There are also fluorescence arguments supporting this interaction as well [17].

3.3 Orientation of 5CB molecules by the nanostructured gold layers

The orientation of liquid crystal produced by different gold layers was analyzed by crossed polarizers and in convergent light (conoscopy) of the obtained cells. The orientation of liquid crystal molecules is always in the vapor incidence plane but the direction and the angle of the tilt depend on the incidence angle and on the thickness of the gold layer. In Figs. 7, images obtained by conoscopy method are given for a cell obtained with the plates P(7) and P(1). Considering the orientation defined in Fig. 2, the LC molecules show in Figs. 7 a slightly inclined orientation of A-type (cell with P(7) plates) or B-type (cell with P(1) plates).

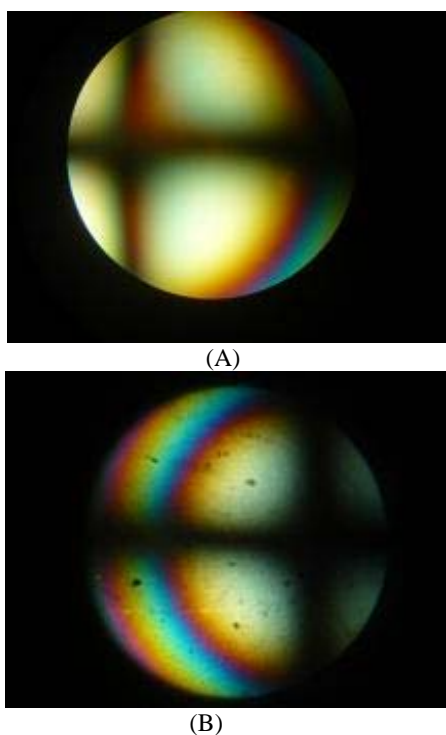


Fig. 7. Conoscopic images of 5CB orientation in the cells having the two plates of a) P(7); b) P(1) batch.

This behavior agrees totally with the influence of the gold topography on the LC alignment. Thus it is known that while the anisotropy in the topography of the gold layer prepared by oblique deposition is subtle, it affords drastic effect on the alignment of liquid crystals. When brought in contact with anisotropic topography of gold nanostructured layer, 5CB assumes a uniform orientation with the principal (long) axis of the mesogens lying in an

azimuthal direction parallel to the direction of minimum roughness of the anisotropic topography [16].

There are still open problems related to the use of these nanostructured gold layers in binding SAMs like aging of the polymer and the instability of these polystyrene layers in watery solutions for long duration, but further studies are necessary to elucidate them.

4. Conclusions

Polystyrene layers were obtained by spin-coating onto glass plates from a toluene solution. Nanostructured gold layers were vacuum deposited at small incidence angle over these PS layers. These gold layers have a rather good adherence to the polystyrene substrate, as tested by an overnight treatment in alcoholic solution: these layers do not peel.

The structure and the thickness of the deposited layers were well characterized. PS layers have of ca. 50 nm while gold layers, 10-20 nm. XRD measurements have shown that gold peaks have the position corresponding to the face-centered cubic structure: However, the peak position and intensity support the idea of a little bit smaller crystallites onto PS than onto glass. XRD reflectometry measurements have given the thickness of the gold layer in good agreement with the value estimated from quartz monitor readings and somehow with the ellipsometric data. In addition, the fit of the ellipsometric data with model function has shown that there is a rather strong interaction between gold atoms and the polystyrene molecules in the substrate.

The nanostructured gold layer deposited onto polystyrene substrate has shown orientational properties as well. Liquid crystal cells made with deposited plates allow to observe a uniform orientation indicating that the long axis of the mesogen molecules most probably lie in a direction parallel to the direction of minimum roughness of the anisotropic topography.

Acknowledgements

The authors thank the financial support of Romanian ministry MEc and of CNMP by the Project VIRNANO/2007 of Research Development and Innovation National Program.

References

- [1] R. G. Nuzzo, D. L. Allara, *J. Amer. Chem. Soc.* **105**, 4481 (1983).
- [2] C. D. Bain, E. B. Troughton, Y.-T. Tao, J. Evall, G. M. Whitesides, R. G. Nuzzo, *J. Amer. Chem. Soc.* **111**, 321 (1989).
- [3] M. D. Porter, T. B. Bright, D. L. Allara, C. E. D. Chidsey, *J. Amer. Chem. Soc.* **109**, 3559 (1987).

- [4] G. M. Whitesides, P. E. Laibinis, *Langmuir* **6**, 87 (1990).
- [5] V. K. Gupta, J. J. Skaife, T. B. Dubrovsky, N. L. Abbott, *Science* **279**, 2077 (1998).
- [6] J. J. Skaife, J. M. Brake, N. L. Abbott, *Langmuir* **17**, 5448 (2001).
- [7] Y.-Y. Luk, M. L. Tingey, D. J. Hall, B. A. Israel, C. J. Murphy, P. J. Bertics, N. L. Abbott, *Langmuir* **19**, 1671 (2003).
- [8] L. A. Tercero Espinoza, K. R. Schumann, Y.-Y. Luk, B. A. Israel, N. L. Abbott, *Langmuir* **20**, 2375 (2004).
- [9] T. Beica, S. Frunza, I. Zgura, L. Frunza, C. Cotarlan, C. Negrila, A. M. Vlaicu, C. N. Zaharia, *J. Optoelectron. Adv. Mater.* submitted (2009).
- [10] Y. Gu, N. L. Abbott, *Phys. Rev. Lett.* **85**, 4719 (2000).
- [11] R. R. Shah, N. L. Abbott, *J. Phys. Chem. B* **105**, 4936 (2001).
- [12] N. L. Abbott, J. J. Skaife, US Patent 6288392 (2001).
- [13] P. N. Sanda, D. B. Dove, H. L. Ong, S. A. Janssen, R. Hoffmann, *Phys. Rev. A* **39**, 2653 (1989).
- [14] S. Frunza, Y. Roques, J. Farenc, D. N. Stoenescu, J. P. Traverse, *Cryst. Res. Technol.* **31**, 1095 (1996).
- [15] S. Frunza, G. Grigoriu, A. Grigoriu, C. Luca, L. Frunza, R. Moldovan, D. N. Stoenescu, *Cryst. Res. Technol.* **32**, 989 (1997).
- [16] J. J. Skaife, N. L. Abbott, *Chem. Mater.*, **11**, 612 (1999).
- [17] G. Carotenuto, A. Longo, L. De Petrocellis, S. De Nicola, P. Repetto, P. Perlo, L. Ambrosio, *Int. J. Nanosci.* **6**, 65 (2007).

*Corresponding author: lfrunza@infim.ro